Unique navigation solution utilizing sky polarization signatures

Laura Eshelman, Adam Smith, Kelsey Smith, David Chenault

Laura M. Eshelman, Adam M. Smith, Kelsey M. Smith, David B. Chenault, "Unique navigation solution utilizing sky polarization signatures," Proc. SPIE 12112, Polarization: Measurement, Analysis, and Remote Sensing XV, 1211203 (3 June 2022); doi: 10.1117/12.2623503

SPIE.

Event: SPIE Defense + Commercial Sensing, 2022, Orlando, Florida, United States

Unique navigation solution utilizing sky polarization signatures

Laura M. Eshelman, Adam M. Smith, Kelsey M. Smith, and David B. Chenault
Polaris Sensor Technologies, Inc., 200 Westside Square, Ste 320, Huntsville, AL, USA 35801-4823

ABSTRACT

With increasing threats to satellites and signal denial methods becoming cheap and effective, GPS failure is a reality and critical risk for navigation, localization, and targeting applications. Inspired by nature, the SkyPASS polarimeter developed by Polaris Sensor Technologies exploits the atmospheric polarization pattern to find highly accurate heading in situations when a typical sun/star sensor would fail to operate. It provides improved availability under cloud cover, under canopy, in urban environments, in civil and nautical twilight, and during sunrise and sunset. Unpolarized sunlight (or moonlight) becomes partially polarized when scattered by atmospheric molecules. Rayleigh scattering creates a polarization pattern, or map, that is unique, depending upon the date, time, and the position of the observer. This natural phenomenon is the scientific basis for SkyPASS operation, and it can be predicted to first order using Rayleigh scattering theory. This paper provides an overview of the SkyPASS polarimeter design, the method to calculate heading from sky polarization information, and the performance of the polarimeter in different environments. The third generation of SkyPASS processes data in real-time and has small enough SWaP to fit almost any platform.

Keywords: Navigation, orientation, Rayleigh scattering, atmospheric polarization, polarimetry, Stokes vector

INTRODUCTION

Military and civilian navigation systems are heavily reliant on GPS technology which has security and availability challenges[1-3]. The absolute angle to target, also known as azimuth or heading, is a critical component required to solve the overall localization/navigation solution; however, in practice, it is difficult to measure with high accuracy in GPS-denied environments. Many solutions utilize relative heading sensors; however, these solutions drift and degrade over time. Calibrating to an absolute heading (sometimes called North finding) is one method to maintain sufficient accuracy to yield high target localization and navigation confidence. Absolute heading can be measured using a digital magnetic compass, with good compasses providing accuracies as low as 5-10 mil; however, they are unreliable due to unpredictable localized variations in the Earth's magnetic field. More accurate heading sensors (reliable to 2-4 mil) usually sacrifice cost, size, weight, power (SWaP-C), or availability and reliability for an increase in accuracy. They may require user leveling, a stationary platform, in-field calibration, and/or a time-to-fix period up to 5 minutes[4,5]. A technology gap exists for an accurate, low SWaP-C sensor that has sufficient reliability, predictability, and availability. Inspired by nature, the SkyPASS polarimeter developed by Polaris[6-8] meets this need by utilizing the polarization map of the sky to calculate highly accurate heading, aiding traditional azimuth sensing methods. Polarized light provides powerful navigation information[9-11] and has been utilized by insects and birds in nature[12-14] and by the Vikings[15].

1.1 Imaging polarimetry

Polarization is a fundamental property of light and enhances traditional sensing methods that measure the brightness and color of a scene. Light is an electromagnetic wave that consists of transverse electric and magnetic fields that oscillate in perpendicular planes with respect to each other (Figure 1). The electric field direction defines the polarization state of light. Light can be linearly, circularly, and randomly polarized. Polarimetry is simply the measurement of the polarization content of a scene and can be accomplished by capturing images at multiple orientations of a linear (or circular) polarizer which acts as a polarization filter. The amount of polarized light that passes through a polarizer depends on the angle between the axis of the polarized light and the axis of the polarized filter. This can be observed using polarized sunglasses and tilting your head (or rotating the glasses) while looking at the sky (Figure 2) since scattered sunlight is polarized.

*Laura.Eshelman@PolarisSensor.com; phone 256-562-0087; fax 256-562-0088; PolarisSensor.com

Polarization: Measurement, Analysis, and Remote Sensing XV, edited by David B. Chenault, Meredith K. Kupinski, Proc. of SPIE Vol. 12112, 1211203 · © 2022 SPIE
0277-786X · doi: 10.1117/12.2623503

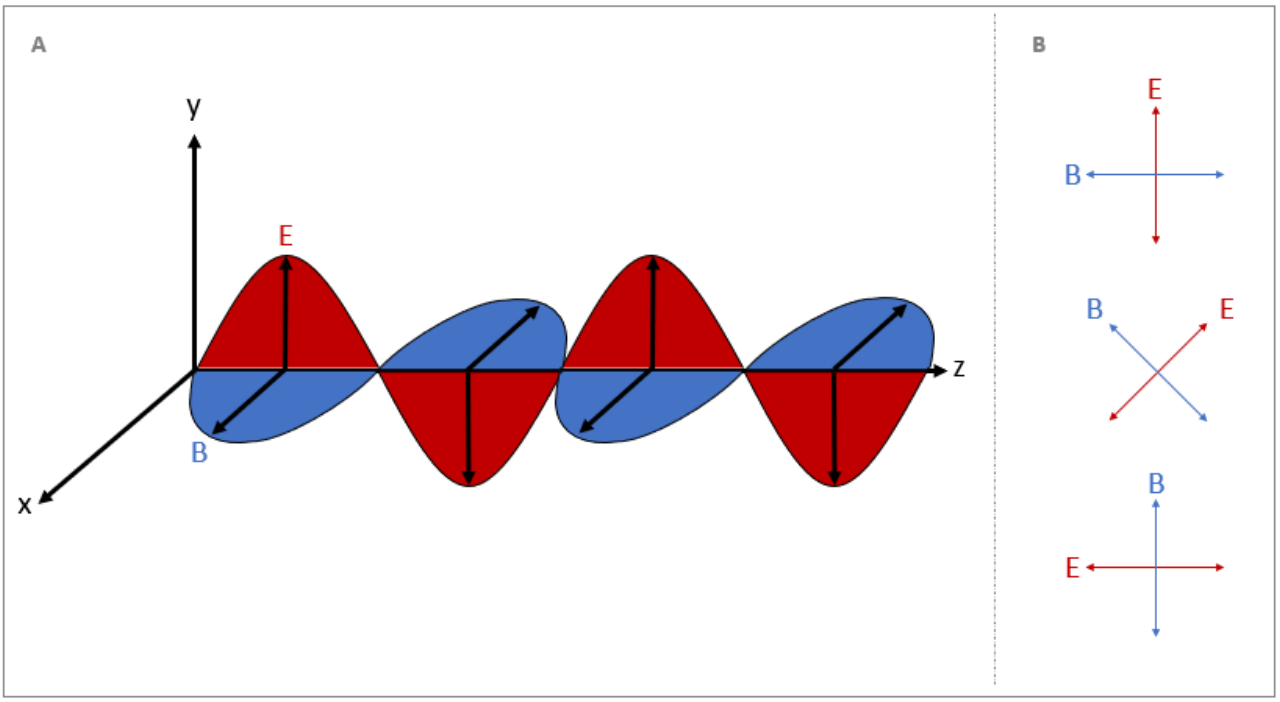

Figure 1. Light is an electromagnetic wave that consists of transverse electric and magnetic fields (A). Light can be linearly (B), circular, or randomly polarized (defined by the electric field direction). Note that circular polarization is rare in nature.

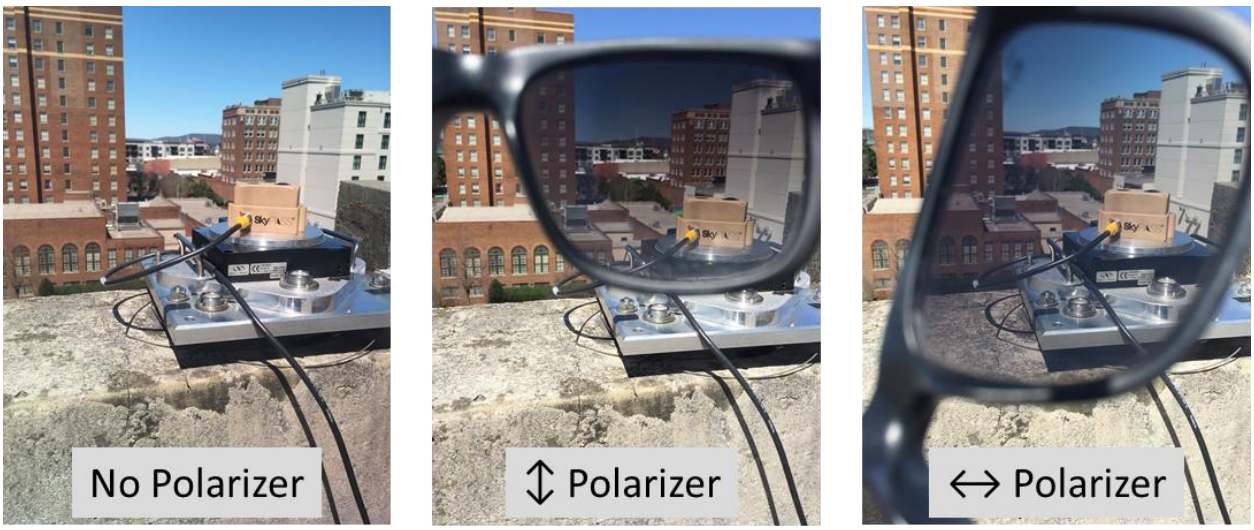

Figure 2. Unpolarized light from the sun becomes linearly polarized when scattered by atmospheric molecules (Rayleigh scattering). Images were collected sequentially at mid-day. Horizontally polarized skylight on the horizon can be blocked using a vertical polarizer (middle). Polarized light can be unblocked when the axis of the polarizer aligns with the polarization state on the horizon (right).

The degree of linear polarization (DoLP) and the angle of polarization (AoP), derived from the Stokes parameters, are two important quantities used to characterize polarization and to calculate heading. In the Stokes vector,

$$\boldsymbol{S} = \begin{bmatrix} S_0 \\ S_1 \\ S_2 \\ S_3 \end{bmatrix} = \begin{bmatrix} \left\langle |E_x|^2 + |E_y|^2 \right\rangle \\ \left\langle |E_x|^2 - |E_y|^2 \right\rangle \\ 2Re\langle E_x E_y{}^* \rangle \\ -2Im\langle E_x E_y{}^* \rangle \end{bmatrix} \propto \begin{bmatrix} I_0 + I_{90} \\ I_0 - I_{90} \\ I_{45} - I_{135} \\ I_L - I_R \end{bmatrix}, \tag{1}$$

Ex and *Ey* are the component electric field amplitudes, and *I* is the radiance collected by the sensor. The subscripts of *I* correspond to the orientation of the linear polarizer. Linear polarization at 0° and 90° are horizontally and vertically polarized, respectively. S_0 represents the overall intensity (radiance), S_1 represents the preference for horizontally polarized light (difference between 0° and 90° polarization), S_2 represents the preference for light polarized at 45° over light polarized at 135°, and S_3 represents the difference between right- and left-hand circular polarized light.

The DoLP represents the percentage of light that is linearly polarized and is defined as

$$DoLP = \frac{\sqrt{{S_1}^2 + {S_2}^2}}{S_0} \tag{2}$$

where a result of 0 indicates unpolarized light and a result of 1 indicates 100% polarized light. Intermediate values represent partially polarized light. Typically, the Stokes vector is normalized meaning S_1 and S_2 range over [-1,1] and $S_0 = 1$.

The AoP is an important quantity that represents the measured orientation of the polarization vector (from 0° to 180°). The AoP can be determined using the Stokes parameters and the following equation:

$$AoP = \frac{1}{2}\tan^{-1}\left(\frac{S_2}{S_1}\right) \tag{3}$$

1.2 Rayleigh scattering; atmospheric polarization

Within Earth's atmosphere, Rayleigh scattering of light causes a defined polarization pattern, which is dependent on the celestial position of the sun (or moon at night) and the relative position and pointing angle of the observer[16,17]. Rayleigh theory, a subset of Mie theory[18], requires that the scattering molecules be small compared to the incident wavelength and that the scattered light experiences a single scattering effect prior to measurement. The scattered light becomes linearly polarized at varying degrees with a particular polarization orientation that depends on the geometry of the source-scatterer-sensor configuration[19-22]. The DoLP of sky polarization can be derived based on the geometry of the source-scatterer-sensor arrangement and is useful for predicting the sky polarization properties. The DoLP relates to the scattering angle (θ), which is the angle between the light's initial direction connecting the sun and target positions and the scattered light's new direction (i.e., from the target position to the sensor). By using Equation 4, the DoLP for any position in the sky can be predicted by knowing the sun, target, and sensor positions while Equation 2 can be used to calculate sky polarization via polarimetric measurements. As expected, viewing the sun directly, which implies no scattering (θ = 0°), results in DoLP = 0 ($S_1 = S_2 = 0$). Similarly, viewing a target position where θ = 90°, results in DoLP = 1 ($S_1 = 1$, $S_2 = 0$,).

$$DoLP = DoLP_{max}\ \frac{1-\cos^2(\theta)}{1+\cos^2(\theta)} \tag{4}$$

$DoLP_{max}$ is a constant that represents the maximum DoLP in the sky at a particular moment and is dependent on atmospheric humidity, aerosols content, optical density, and time of day.

On clear days at either sunrise or sunset, a maximum band of polarization extends from the horizon through the zenith, approximately 90° from the sun (Figure 3). In general, the sky DoLP increases from the sun to the maximum band of polarization, then decreases towards the anti-sun position. The maximum band of polarization shifts based on the position of the sun. Therefore, at mid-day when the sun is high in the sky, sky polarization observed at the zenith is minimal[23-27]. Multiple scattering from aerosols[28-30], clouds[31-35], and the underlying surface[36] can reduce the degree of polarization; however, the direction of polarization remains similar for clear and slightly overcast skies[31-35]. The AoP direction is normal to the scattering plane which contains the sun, target, and sensor and for any given time, sensor position, and target position in the sky, the AoP can be predicted based solely on the geometry on the situation.

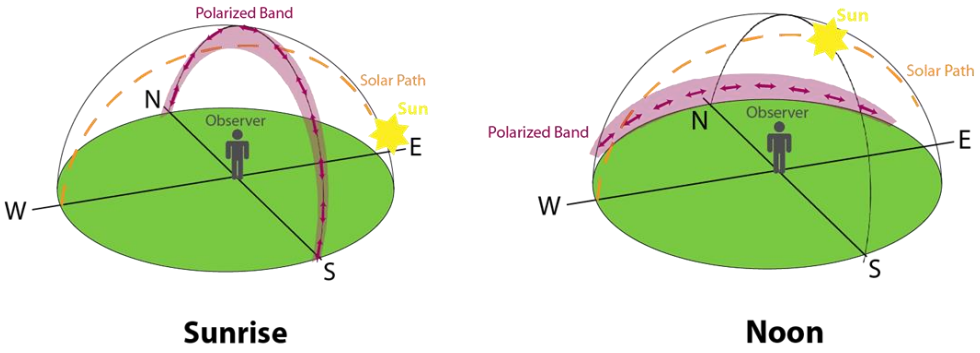

Figure 3. Sky polarization illustration of the max band of polarization and direction of polarization at sunrise and at noon.

Simulated AoP and DoLP stereographic projections of the sky at sunrise and at mid-day, with the sun directly on the horizon and above the observer are shown in Figure 4. In the simulated images, zenith is at the center and the circumference represents positions along the horizon. In general, the DoLP increases as one moves away from the sun until it reaches a maximum at $\theta = 90°$ and then it decreases back to zero at the anti-sun position. In the AoP image, a symmetric pattern is observed, with a line connecting both the sun and the zenith. For navigation purposes, this map is more informative than the DoLP image because a complete hemispherical image is not required to determine the position of the sun, which relates to the pointing direction of the platform.

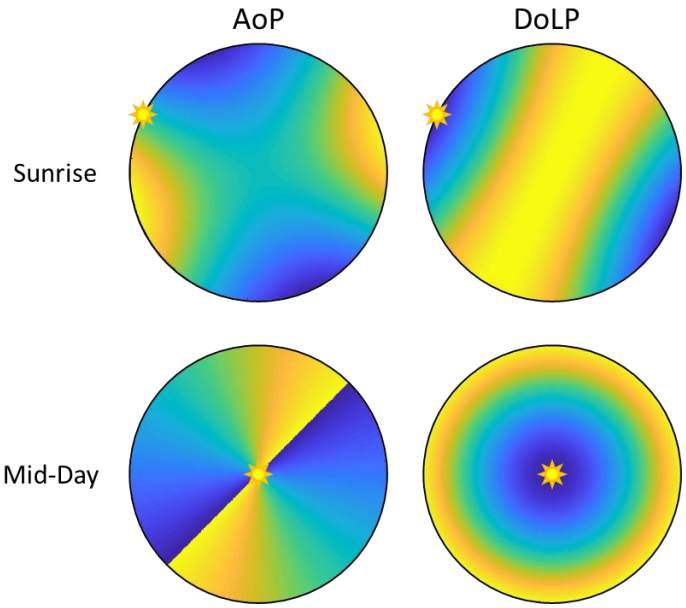

Figure 4. Simulated AoP and DoLP stereographic projections of the sky at sunrise and at noon, with the sun directly on the horizon and above the observer, respectively. Results are representative of collecting measurements in Havana on June 20th. In the DoLP image, yellow represents maximum polarization, where dark blue represents zero polarization.

2. SENSOR DESCRIPTION

The SkyPASS polarimeter is a visible imaging polarimeter that measures the first three Stokes parameters (S_0, S_1, S_2) at the zenith. It employs a division of focal plane architecture with three lens arrays (channels) projecting a target scene to separate locations on the focal plane array (FPA). Each channel contains a uniquely oriented linear polarizer resulting in three individual polarized images. The sensor is polarimetrically calibrated prior to measurements using an integrating sphere and a calibration polarizer (placed in front of the objective and made to rotate in 5° increments). The calibration procedure results in a data reduction matrix through which the three measured polarization images are mapped to determine the pixel resolved DoLP and AoP. The SkyPASS polarimeter is environmentally designed to IP67.

SkyPASS Gen3 has an embedded processor and collects data in real-time at 1Hz. The daytime integration time for the polarimeter ranges from 5ms to 30ms depending on design considerations for field of view and twilight optimization. The maximum integration time is 1600ms. The operation of the polarimeter is limited to tilt angles less than 13° due to the field of view of the sensor (an out of bound error message will occur for tilt measurements beyond the limit). The performance of the SkyPASS polarimeter is characterized using a surveyed rotation plate, and machined tilt plates are used to evaluate the performance of the polarimeter at different tilt angles.

Algorithms to detect and decipher the polarization map of the sky can be utilized to compute highly accurate heading based on knowing date, time, and the user position. The confidence metric reported is determined based on the sky and lighting conditions.

Figure 5. The SkyPASS polarimeter opto-mechanical design (left) has a size and weight of 1.5” x 1.5” x 1.2” and 1.76oz, respectively. When included with a sun tracker, embedded processing, and ruggedized housing (Gen3), the SWaP becomes 3.5” x 1.9” x 2.4”, 8oz, and 4.1W, respectively. The performance of the SkyPASS polarimeter is characterized using a surveyed rotation plate.

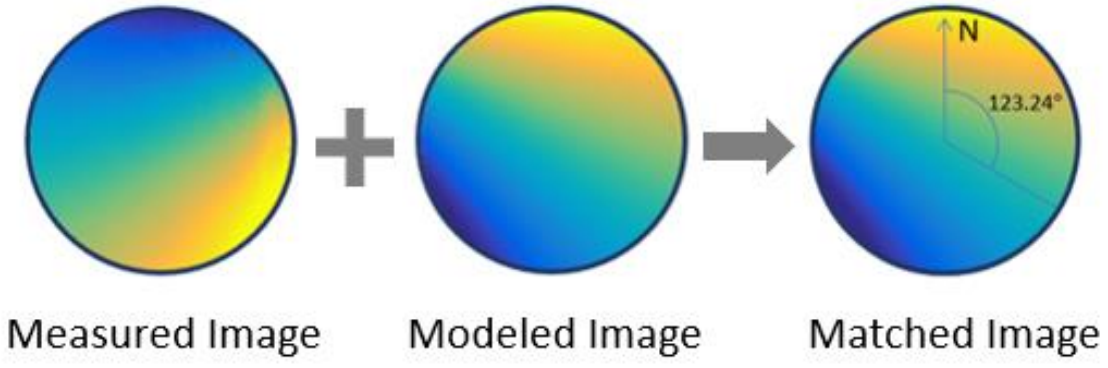

Figure 6. Heading calculation steps: take a measurement of the sky, predict the polarization using known date, time, pitch, roll, and user position, and rotate the measured image to match the model.

3. OPERATIONAL CAPABILITIES

The objective for the SkyPASS polarimeter is to provide 24-hour, all weather operation. System capabilities and limitations in GPS-denied environments, clear and cloudy skies, in twilight, at night, and in dynamic operation are presented in the subsequent subsections. For reference, example sky conditions are shown in Figure 7.

Figure 7. Example of clear skies (top), partial cloud cover (middle-top), heavy cloud cover (middle-bottom), and twilight (bottom) test conditions.

3.1 GPS-Denied Operation

To find North (heading) from sky polarization measurements, the date, time, and the position of the user must be known. The accuracy of the SkyPASS polarimeter directly relates to the input position error and input time error. Simulated results when varying input error for position and time are provided in Table 1 and Table 2, respectively. These results were determined by analyzing a solar position calculator, accurate to within 0.0003° or ~0.0052mil. Results in Table 1 represent a GPS-denied scenario where sensors are unable to update the sensor position to accommodate the loss of GPS. Distances representing position errors were measured in longitude, as they had a larger impact on heading measurement error. The results depend on the distance to the solar ecliptic. This scenario was done for the spring equinox, so the ecliptic is on the equator. As observed in Table 1, higher latitudes near the poles will yield larger overall errors.

Table 1. Comparison of heading measurement error versus position error for three latitudes and varying times of day. These results assume accurate GPS time.

	Heading Measurement Error (mil)					
Latitude (°)	**10**		**34.73***		**80**	
Distance (m)	**Noon**	**Sunset**	**Noon**	**Sunset**	**Noon**	**Sunset**
0	0	0	0	0	0	0
10	0.009	<0.005	<0.005	<0.005	0.009	0.009
100	0.091	<0.005	0.178	0.011	0.178	0.089
1000	0.912	0.028	0.334	0.109	0.917	0.889
10000	9.117	0.277	3.344	1.087	9.167	8.892

*Huntsville, Alabama

In Table 2, the same set of circumstances were tested, but instead of testing various distances, various time differences were studied. This represents losing a precise time estimate from GPS signals. The results in Table 2 show that even 10s of error for specific cases will impact the performance of the SkyPASS polarimeter. Thus, when losing GPS signal, the SkyPASS polarimeter would need a clock to sustain the GPS time to within 1 seconds for the life of the expected operation. Overall, the results show that an input accuracy for position less than 0.5km and an input accuracy for time less than 1s shall have no measurable impact on the accuracy of the SkyPASS polarimeter (0.1° or 1.78mils).

Table 2. Comparison of heading measurement error versus position error for three latitudes and varying times of day. These results assume accurate GPS position.

	Heading Measurement Error (mils)					
Latitude (°)	**10**		**34.73***		**80**	
Time Error (mm:ss)	**Noon**	**Sunset**	**Noon**	**Sunset**	**Noon**	**Sunset**
00:00	0	0	0	0	0	0
00:01	0.417	0.013	0.127	0.041	0.074	0.072
00:10	4.165	0.126	1.275	0.414	0.738	0.716
00:30	12.496	0.377	3.825	1.241	2.215	2.149
01:00	24.988	0.753	7.65	2.483	4.431	4.297

*Huntsville, Alabama

3.2 Cloud Cover Operation

Full-image algorithms to select regions of the sky to calculate heading would improve the overall performance of the SkyPASS polarimeter. Developing and implementing full-image algorithms is in-progress. Figure 8 shows imagery collected with no cloud cover. The left image shows the S_0 data product, which is equivalent to a standard visible image (shown with a spectrum colormap). Here, the sun is just off the image to the top, and white represents brighter pixels with blues, purples, and blacks representing darker pixels. The center and right images are DoLP and AoP, respectively. The DoLP and AoP images show reasonable gradients and patterns as predicted by Rayleigh scattering models for clear (though somewhat hazy) sky conditions.

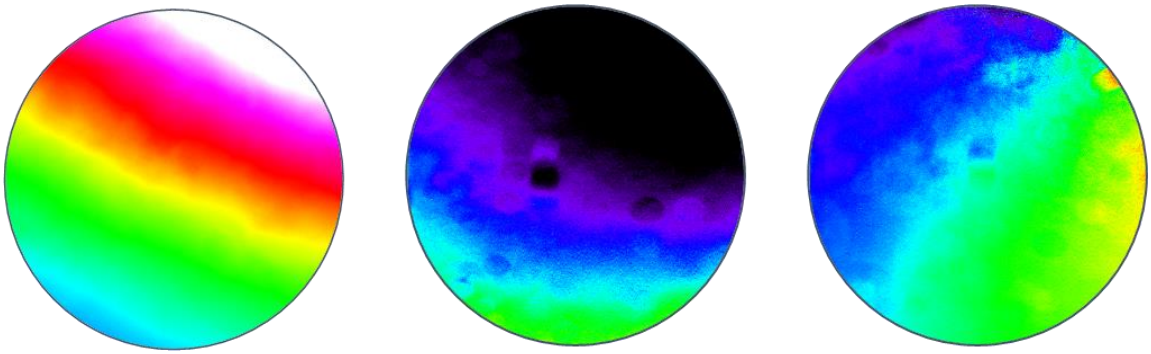

Figure 8. Visible S_0 (left), DoLP (middle), and AoP (right) imagery of clear sky conditions. The dark colors represent lower DoLP.

Figure 9 shows the same sky location taken within 10 minutes of Figure 8, but now with a large, dense, cumulus cloud persisting over the top half of the image (as seen in the left visible image). In the current polarimeter configuration, the polarization channels have set integration times which cause the cloud portions of the sky to be soaked (or set to the highest signal value). This limits the sensor and causes the calculations in those pixel areas to become unreliable (which is accounted for in the confidence metric). For some cases, it's better to adjust the integration time so that the clouds are not soaked (overcast skies; thin cirrus clouds). Because water vapor has a depolarizing effect and no preferential scatter, the DoLP is greatly diminished by clouds, but the AoP pattern remains as predicted for most cloudy conditions (if it is resolvable)[31-35.] Ice crystals and large water droplets in the atmosphere do have different polarization effects, making AoP values significantly different from those predicted using Rayleigh scattering theory. If the DoLP is reduced due to multiple scattering from a cloud, the accuracy of the SkyPASS polarimeter degrades; however, when the AoP pattern changes due to water clouds, the accuracy of the SkyPASS polarimeter is unreliable. These results indicate that a more robust, full-image algorithm that selects clear-sky regions to calculate heading is required for operation in partly cloudy skies.

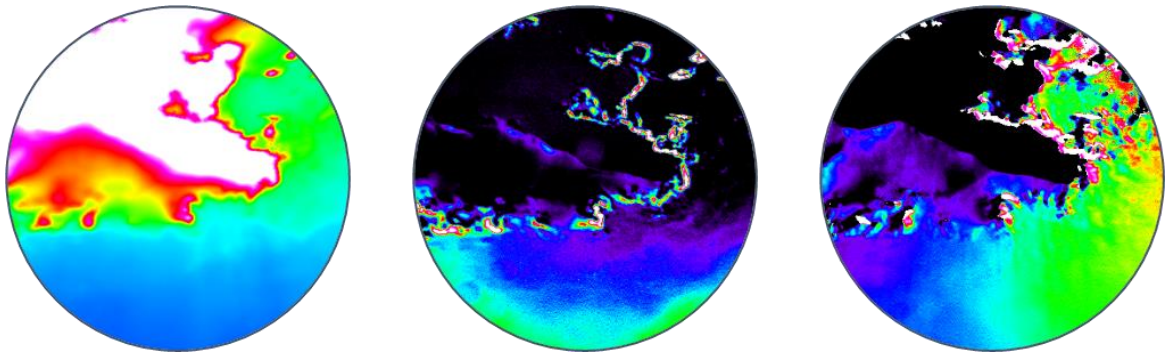

Figure 9. Visible S_0 (left), DoLP (middle), and AoP (right) imagery of a dense, cumulus cloud in top portion of the image. The dark colors represent lower DoLP.

3.3 Sunrise/Sunset and Night Operation

The SkyPASS polarimeter has the best performance during sunrise and sunset which is when traditional sun, moon, and star tracking solutions fail. Either the sky is too bright for star tracking or the sun/moon have not yet cleared the horizon or terrain. The polarimeter can collect accurate data until about 30 minutes before sunrise and after sunset (civil twilight). At this point, the light level and the signal-to-noise ratio become too low to achieve reasonable sky polarization measurements. The maximum allowed integration time configured for the polarimeter is 1600ms. More flexibility in integration time/gain adjustment and changes to the optical design have shown that accurate measurements can be extended beyond civil twilight; however, physical limitations due to scattered skylight and moonlight interactions exist where the AoP pattern has been observed to become random and not predictable in nautical/astronomical twilight[37]. Thus far the limiting factor for SkyPASS at twilight has been getting enough light.

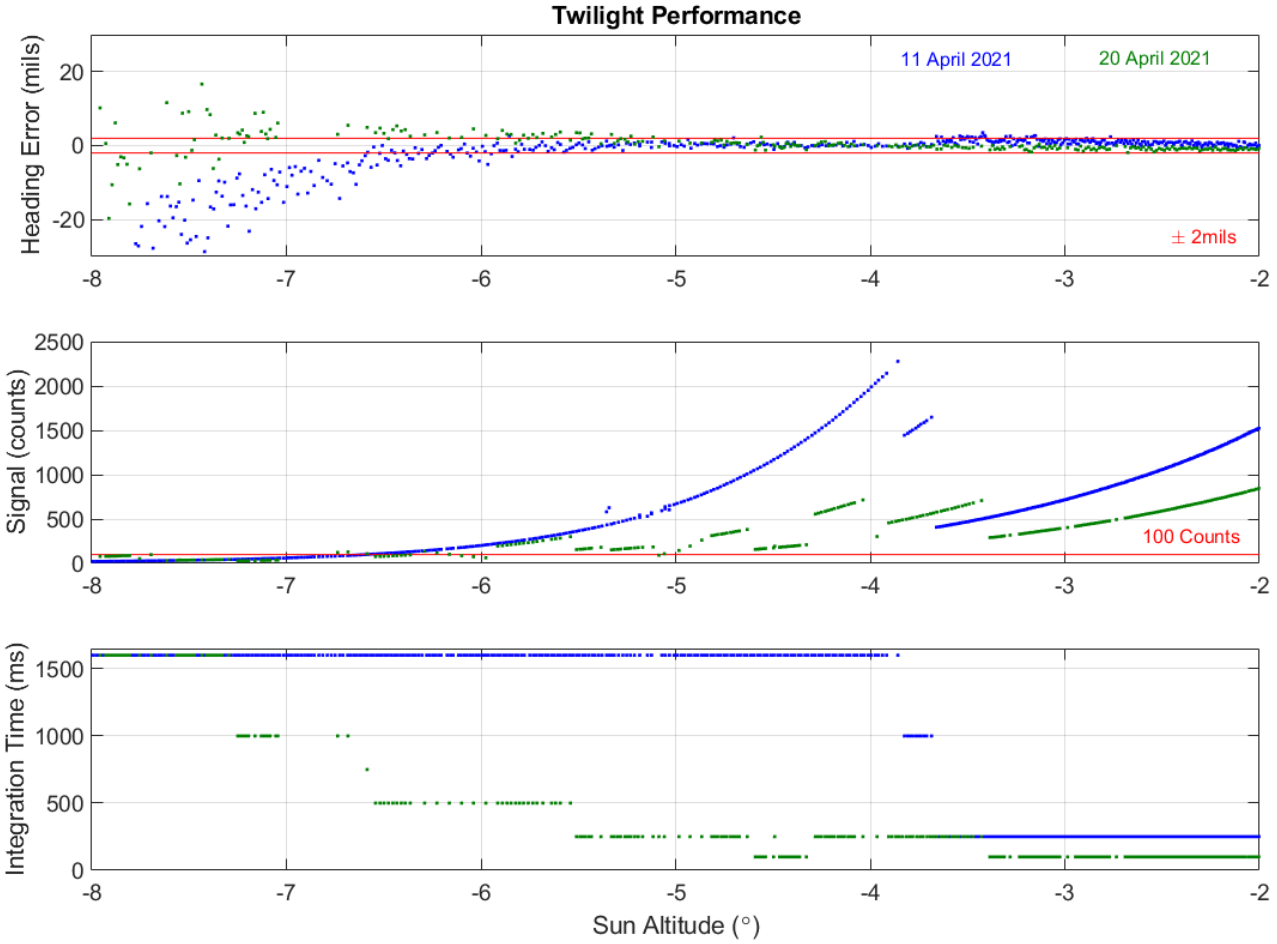

Figure 10. The performance of the SkyPASS polarimeter in twilight.

To achieve 24-hour operation, SkyPASS must be capable of handling nighttime environments. Polarization of the nighttime sky is primarily dominated by the following sources in order of their contribution: the moon, stars and planets, the Milky Way, zodiacal light, and airglow[37,38]. The most dominant contributor is the moon, and the moon represents the only nighttime source which has been shown to produce a measurable polarization pattern like the sun during the daytime. In Gal et al.[37], a comparison of moonlit and sunlit skies is provided. As is expected due to the lower light levels, the moonlit sky pattern is much noisier than the sunlit pattern. However, the pattern does exist and does appear to be the same pattern as seen in the sunlit sky.

Polaris is currently investigating the capability of the SkyPASS polarimeter at night. One important note is that larger integration times (>10s) are required since moonlight is about 463,000 weaker than sunlight[39]. We expect at minimum an increase measurement delay (due to high integration times) in addition to a decrease in accuracy of SkyPASS at night. Additionally, in urban environments, artificial light glow from street and building/house lights is a major contributor to the nighttime scattered light. As seen in Kyba et. al., this light negatively affects the observed polarization pattern[40]. The DoLP dictates the accuracy of the AoP, which is used by SkyPASS, with higher DoLP values representing greater measurement accuracy of AoP. In Kyba et. al., DoLP of 57% in the daytime was measured compared to 29% of rural nighttime at full moon. However, this DoLP drops to 11% in urban nighttime at full moon. Thus, it is likely that the SkyPASS polarimeter will not provide sufficient measurement accuracy at nighttime in urban environments with high light pollution. In addition, it may be difficult to measure a polarization signature for navigation on moon-less nights[41].

3.4 Dynamic Operation

The performance of the SkyPASS polarimeter degrades in dynamic operation as observed in Figure 11. For the results presented, the polarimeter collected frames with no averaging and a KVH inertial sensor was used as truth for heading and to feed the sensor date, time, latitude, and longitude. In general, performance improves with frame averaging (benefit for static applications). With no averaging, the temporal noise is 0.64mil; with averaging 8 frames, the temporal noise is 0.27mils. Through testing, the vehicle direction varied; therefore, any time delay between SkyPASS heading measurements and the reference while the vehicle heading was changing would appear as an error. Thus, time syncing between measurements and grabbing pitch and roll mid-exposure may improve results. Changes to the embedded software architecture are in-progress to improve dynamic operation.

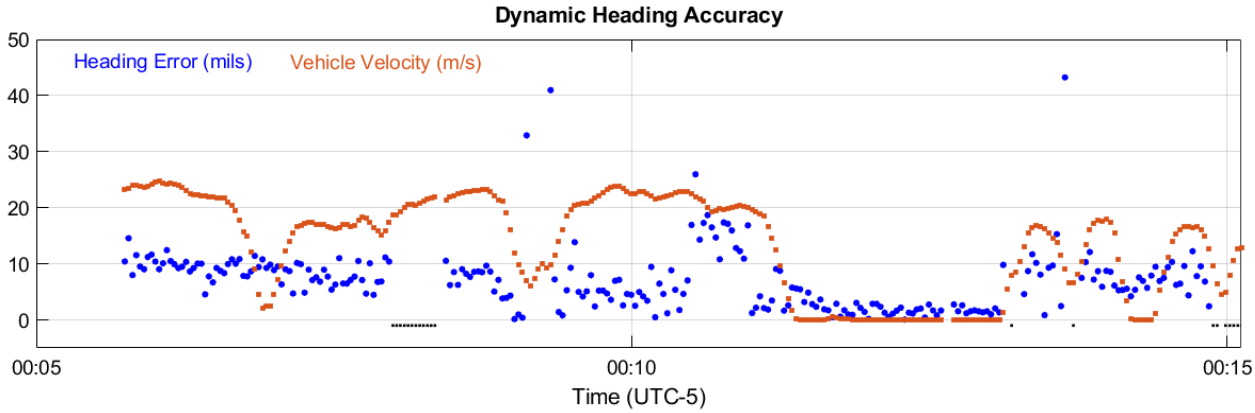

Figure 11. Dynamic heading accuracy for a series of measurements collected in Huntsville, Alabama on 9 September 2021 using a ground-based vehicle. Measurements correspond to sun altitudes ranging from -0.8° to -3.3° and a KVH inertial sensor was used as truth for heading.

3.5 Overall Operation

The ideal operation to achieve accuracy of less than 2mils with the SkyPASS polarimeter is between sun altitudes of -4° and 35° in clear, non-overcast skies and in static operation. The performance of the SkyPASS polarimeter degrades in cloudy conditions and for higher sun altitudes when only measuring sky polarization at the zenith. This can be observed in Figure 12 where degraded performance corresponds to lower DoLP values. A polarimeter that utilizes full-image algorithms has the capability to select regions of interest (ROIs) with high DoLP values, leading to more accurate solutions. Polaris is improving SkyPASS' software and algorithms to achieve this type of operation. In addition to low DoLP, degraded performance can correspond to saturation of signals from clouds or lack of signal during sunrise/sunset. In the current configuration, the SkyPASS polarimeter can achieve a higher accuracy and better availability with a reduced FOV of the sky; however, by reducing the FOV, the tilt capability of the sensor is limited. There is a tradeoff between performance versus operational platform orientation. By implementing full-image algorithms, expanding tilt capability beyond 13° may be achievable.

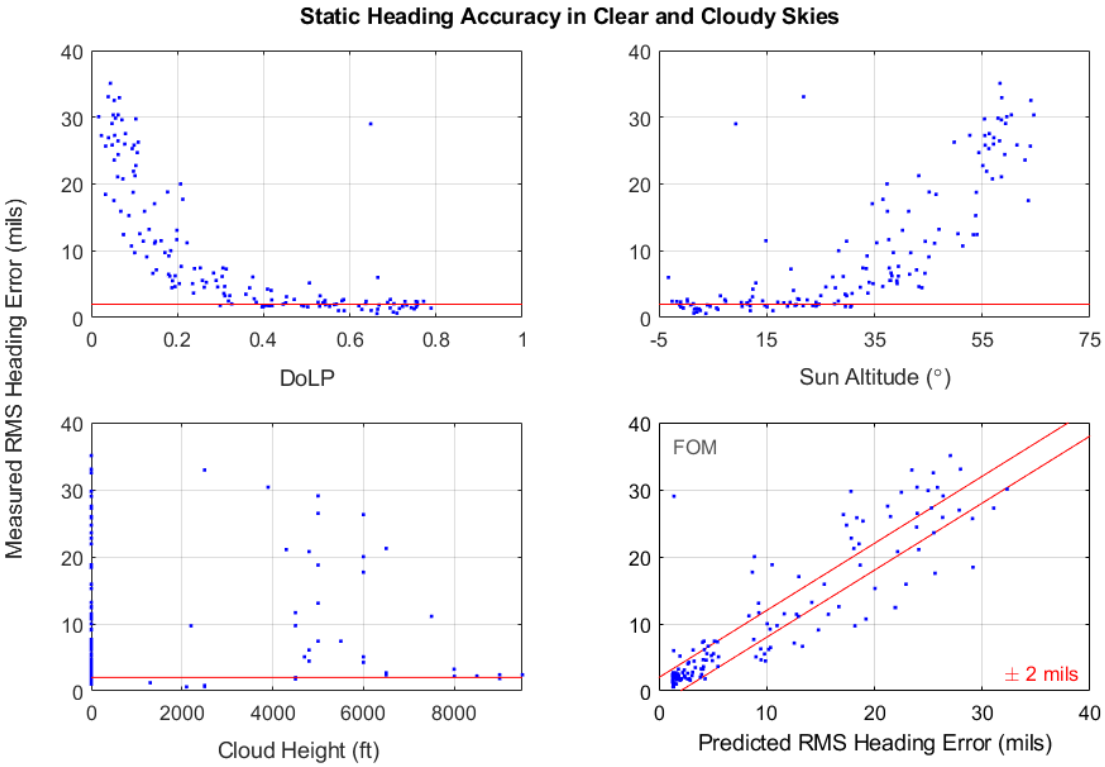

Figure 12. Multi-sensor performance in clear/cloudy sky conditions with measurements collected over multiple days/months at the zenith. Measurements represent the RMS heading error of 24 measurements collected in 15° increments using a surveyed rotation stage. METAR cloud data was retrieved from the weather station at the Huntsville airport (KHSV).

Figure 13. SkyPASS testing in clear to cloudy skies, on different platforms, and in different locations.

4. CONCLUSION

Inspired by nature, the SkyPASS polarimeter exploits the atmospheric polarization pattern to find highly accurate heading. Sky polarization patterns provide strong gradient information describing the absolute heading of the sensor. Navigation via measuring sky polarization complements traditional methods by greatly increasing availability while being unaffected by magnetic anomalies, by being immune to GPS-inhibiting techniques, and by not requiring leveling or initialization. Operation at sunrise, sunset, and during cloudy days is possible, even at accuracies that still outperform current celestial, inertial, and vision-based methods. Degraded performance is observed in heavy cloud cover and in dynamic conditions. Nighttime polarization has been demonstrated as an orientation method in the animal kingdom; however, while theoretically possible and achievable in a contrived setup (nonmoving platform, long integration times, non-urban environment, etc.), nighttime sky polarization sensing is unlikely to significantly outperform other nighttime heading sensing methods. Star and moon tracking would be a better solution during nighttime operation due to the motion limitations set by sky polarization.

REFERENCES

[1] Simsky, M., "How do we ensure GNSS security against spoofing?," GPS World, 9 October 2019, <https://www.gpsworld.com/how-do-we-ensure-gnss-security-against-spoofing/> (2020).

[2] Evans, G., "The problem with GPS in the modern military," Army Technology, 20 January 2020, < https://www.army-technology.com/analysis/the-problem-with-gps/ > (2020).

[3] "GPS drift and environmental factor impact on GPS accuracy" <https://support.garmin.com/en-US/?faq=CC5azODuBd9BhRbKvp82JA> (2021).

[4] Mao, N., Xu, J., Li, J., and He, H., "A LSTM-RNN-based fiber optic gyroscope drift compensation", Mathematical Problems in Engineering, (2021) HTTPS://DOI.ORG/10.1155/2021/1636001.

[5] <https://www.vectornav.com/resources/inertial-navigation-primer> (2021).

[6] Aycock, T., Chenault, D., Lompado, A., and Pezzaniti, J. L., "Sky polarization and sun sensor system and method," U.S. Patent 9 423 484, (2016).

[7] Aycock, T., Lompado, A., and Wheeler, B., "Using atmospheric polarization patterns for azimuth sensing," Proc. SPIE 9085, Sensors and Systems for Space Application VII, 90850B (2014) HTTPS://DOI.ORG/10.1117/12.2054107.

[8] Smith, A. M., Pezzaniti, J. L., Chenault, D. B., and Lompado, A., "Study of natural down-welling sky light with imaging spectro-polarimeter," Proc. SPIE 10655, Polarization: Measurement, Analysis, and Remote Sensing XIII, 106550M (2018). https://doi.org/10.1117/12.2310007.

[9] Guan, G., Gu, J., and Wu, M., "The novel method of north finding based on the skylight polarization," J. Eng. Sci. Tech. Rev., 6(1), 107-110 (2013).

[10] Sarkar, M., San Segundo Bello, D., van Hoof, C., and Theuwissen, A., "Biologically inspired autonomous agent navigation using an integrated polarization analyzing CMOS image sensor," Proc. Eng., 5, 673-676 (2010).

[11] Karman, S.B., Diah, S.Z.M, and Gebeshuber, I.C., "Bio-inspired polarized skylight navigation sensors: A review," Sensors, 12, 14232-14261 (2012).

[12] Mathejczyk, T., and Wernet, M., "Sensing polarized light in insects'" Oxford Research Encyclopedia of Neuroscience, (2017) HTTPS://DOI.ORG/10.1093/ACREFORE/9780190264086.013.109.

[13] Dacke, M., Nordström, P., and Scholtz, C. H., "Twilight orientation to polarised light in the crepuscular dung beetle *Scarabaeus zambesianus*," *J Exp Biol*, 206 (9): 1535–1543 (2003). https://doi.org/10.1242/jeb.00289.

[14] Sakura, M., Lambrinos, D., and Labhart, T., "Polarized skylight navigation in insects: model and electrophysiology of e-vector coding by neurons in the central complex," J Neurophysiol, 99(2):6, 67-82 (2008).

[15] Barta, A., Farkas, A., Száz, D., Egri, Á., Barta, P., Kovács, J., Csák, B., Jankovics, I., Szabó, G., and Horváth, G., "Polarization transition between sunlit and moonlit skies with possible implications for animal orientation and Viking navigation: anomalous celestial twilight polarization at partial moon," Appl Opt., 53(23):5, 193-204 (2014).

[16] Strutt, J., "On the light from the sky, its polarization and colour," Philosophical Magazine, Vol. 41 (4), 107-120 (1871).

[17] Strutt, J, "On the transmission of light through an atmosphere containing small particles in suspension, and on the origin of the blue of the sky," Philosophical Magazine, Vol. 47 (5), 375-393, (1899).

[18] Fu, Q., and Sun, W., “Mie theory for light scattering by a spherical particle in an absorbing medium,” Applied Optics, V. 40(9), 1354-1361, (2001).

[19] Van de Hulst, H.C., [Light Scattering by Small Particles], Dover Publications, New York, Chap. 6 and 7, (1981).

[20] Können, G. P., [Polarized Light in Nature], Cambridge University, (1985).

[21] Bohren, C. F., and Huffman, D. R., [Absorption and Scattering of Light by Small Particles], John Wiley and Sons, Inc., New York, 130-136 (1998).

[22] Coulson, K. L., [Polarization and Intensity of Light in the Atmosphere], Deepak Publishing, (1988).

[23] Gal J., Horváth, G., Meyer-Rochow, V.B., and Wehner, R, “Polarization patterns of the summer sky and its neutral points measured by full-sky imaging polarimetery in Finnish Lapland north of the Arctic Circle,” in Proc. R. Soc. Lond. A, 1385 –1399 (2001).

[24] Lee, R. L,“Digital Imaging of clear-sky polarization,” App. Opt., 37(9), 1465- 1476 (1998).

[25] Miyazaki, D., Ammar, M., Kawakami, R., and Ikeuchi, K., “Estimating sunlight polarization using a fish-eye lens,” IPSP Journal, 49(4), 1234-1245 (2008).

[26] Eshelman, L. M., and Shaw, J. A., "Visualization of all-sky polarization images referenced in the instrument, scattering, and solar principal planes," Opt. Eng. 58(8) 082418 (2019) HTTPS://DOI.ORG/10.1117/1.OE.58.8.082418.

[27] H. Zhao, W. Xu, Y. Zhang, X. Li, H. Zhang, J. Xuan, and B. Jia, “Polarization patterns under different sky conditions and a navigation method based on the symmetry of the AOP map of skylight,” Opt. Express 26, 28589–28603 (2018).

[28] Boesche, E., Stamnes, P., Ruhtz, T., Preusker, R., and Fischer, J., “Effect of aerosol microphysical properties on polarization of skylight: sensitivity study and measurements,” Appl. Opt.45, 8790–8805 (2006).

[29] Kreuter, A., Emde, C., and Blumthaler, M., “Measuring the influence of aerosols and albedo on sky polarization,” Atmos. Res. 98, 363–367 (2010).

[30] Eshelman, L. M., and Shaw, J. A., “The VIS-SWIR spectrum of skylight polarization,” Appl. Opt.57, 7974–7986 (2018).

[31] Pust, N. J., and Shaw, J. A., “Digital all-sky polarization imaging of partly cloudy skies,” Appl. Opt. 47, H190–H198 (2008).

[32] Hegedus, R., Akesson, S., and Horváth, G., “Polarization patterns of thick clouds: overcast skies have distribution of the angle of polarization similar to that of clear skies,” J. Opt. Soc. Am. A, 24(8), 2347- 2356 (2007).

[33] Eshelman, L. M., Tauc, M. J., and Shaw, J. A., “All-sky polarization imaging of cloud thermodynamic phase,” Opt. Express 27, 3528–3541 (2019).

[34] Pomozi, I., Horváth, G., and Wehner, R., “How the clear-sky angle of polarization pattern continues underneath clouds: full-sky measurements and implications for animal orientation,” J. Exp. Biol. 204, 2933–2942 (2001).

[35] Horváth, G., Barta, A., Gál, J., Suhai, B., and Haiman, O., “Ground based full-sky imaging polarimetry of rapidly changing skies and its use for polarimetric cloud detection,” Appl. Opt.41, 543–559 (2002).

[36] Dahlberg, A. R., Pust, N. J., and Shaw, J. A., “Effects of surface reflectance on skylight polarization measurements at the Mauna Loa Observatory,” Opt. Express19, 16008–16021 (2011).

[37] Barta, A., Farkas, A., Száz, D., Egri, A., Barta, P., Kovács, J., Csák, B., Jankovics, I., Szabó, G., and Horváth, G., "Polarization transition between sunlit and moonlit skies with possible implications for animal orientation and Viking navigation: anomalous celestial twilight polarization at partial moon," Appl. Opt. 53, 5193-5204 (2014)

[38] Gal, J., Horváth, G., and Barta, A., "Polarization of the moonlit clear night sky measured by full-sky imaging polarimetry at full Moon: Comparison of the polarization of moonlit and sunlit skies," Journal of Geophysical Research, Vol. 106, No. D19, pp. 22,647-22,653, 2001.

[39] Shaw, J. A., "The digital blue sky at night," Optics & Photonics News, 16, (2005).

[40] Kyba, C., Ruhtz, T., Fischer, J., and Holker, F., "Lunar skylight polarization signal polluted by urban lighting," Journal of Geophysical Research, Vol. 116, D24106, 1-7, (2011).

[41] Hopkin, M., "Dung beetles push the light of the Moon," Nature, (2003).